Functionally linked amygdala and prefrontal cortical regions are innervated by both single and double projecting cholinergic neurons

Bence Barabás[1,2,4], Zsófia Reéb[1,3], Orsolya I. Papp[1] and Norbert Hájos[1,4,5]

[1] HUN-REN Institute of Experimental Medicine, 1083, Budapest, Hungary

[2] János Szentágothai School of Neurosciences, Semmelweis University, 1085, Budapest, Hungary

[3] Doctoral School of Biology, Institute of Biology, ELTE Eötvös Loránd University, 1117 Budapest, Hungary

[4] The Linda and Jack Gill Center for Molecular Bioscience, Indiana University Bloomington, 47405, Indiana, USA

[5] Program in Neuroscience, Department of Psychological and Brain Sciences, Indiana University Bloomington, 47405, Indiana, USA

Correspondence should be addressed to
Norbert Hajos

nhajos@iu.edu

Acknowledgements: We acknowledge financial support from the Hungarian Brain Research Program (2017-1.2.1-NKP-2017-00002) and National Research, Development and Innovation Office (K131893 and RRF-2.3.1-21-2022-00004). The authors are grateful to Éva Krizsán and Erzsébet Gregori for their excellent technical assistance. We also thank László Barna, the Nikon Microscopy Center at the Institute of Experimental Medicine, Nikon Austria GmbH, and Auro-Science Consulting, Ltd., for kindly providing microscopy support.

ABSTRACT

Cholinergic cells have been proposed to project simultaneously to those cortical areas that are mutually interconnected with each other. We tested this hypothesis by investigating the cholinergic innervation of functionally linked cortical regions: the basal amygdala nucleus (BA) – dorsal part of the medial prefrontal cortex (dmPFC) and the basomedial amygdala nucleus (BMA) – ventral part of the mPFC (vmPFC). Using retrograde tracing, we found that basal forebrain cholinergic neurons projecting to the BA and BMA were in the ventral pallidum/substantia innominata (VP/SI) and horizontal limb of the diagonal band of Broca (HDB), respectively. Anterograde viral tracing confirmed that VP/SI cholinergic neurons preferentially targeted the BA and dmPFC. In contrast, HDB cholinergic cells innervated the BMA and vmPFC. We also demonstrated that a portion of cholinergic neurons projected both to the amygdala and mPFC. Furthermore, we revealed that the vesicular glutamate transporter type 3 (VGLUT3) was present typically in cholinergic boutons in the BA but not BMA, whereas their vesicular GABA transporter (VGAT) content could not be detected in adult mice. Our data thus revealed that cholinergic innervation of the dmPFC-BA and vmPFC-BMA originates from two distinct neuronal populations, which innervate interconnected target regions in a mutually exclusive manner. The dual innervation strategy, i.e., the existence of cholinergic cell populations with single as well as simultaneous projections to the amygdala and mPFC, provides the possibility for both synchronous and independent control of the operation in these cortical areas, a structural arrangement that may maximize computational support for functionally linked regions.

Significance statement. This study reveals the logic how basal forebrain cholinergic neurons innervate two functionally linked cortical regions, the dmPFC-BA and vmPFC-BMA, mutually interconnected circuits that have been shown to be involved in controlling opposing fear states and behavior. Our findings demonstrate that the VP/SI and HDB innervate dmPFC-BA and vmPFC-BMA networks, respectively. Cholinergic cells project primary either to the mPFC or to the amygdala, but there is a population of cholinergic neurons that sends axon collaterals to both areas. This structural organization allows for simultaneous and independent control of operation, maximizing computational support for cortical processing. The two types of cholinergic control

of fear-related cortical areas can be a significant research target at various fear learning deficits, such as PTSD.

INTRODUCTION

Recognizing threats is essential for animal survival. Therefore, it is not surprising that many brain circuits contribute to the detection of dangerous situations, leading to the elevation of attentive and affective state linked to the threat (Davis, 1997; Izquierdo et al., 2016; Ledoux, 2000; Tovote et al., 2015). This challenge-triggered mental state helps to generate the most appropriate behavioral response, aiming to avoid, or at least, reduce any potential harm as well as forming memory that can guide future avoidance of similar threat. These complex brain processes are regulated at different levels in the nervous system. Top-down control is provided by cortical circuits located in the basolateral amygdala and medial prefrontal cortex (mPFC), areas which are reciprocally connected with each other (Burgos-Robles et al., 2009; Herry et al., 2008; Little & Carter, 2013; Sotres-Bayon et al., 2012; Weiskrantz, 1956). These two structures can be parceled based on their connectivity and role playing e.g., in the generation of negative emotional states (Lacroix et al., 2000; Ledoux, 2000). The basal nucleus of the amygdala (BA) and the dorsal part of the mPFC (dmPFC), including the prelimbic and anterior cingulate cortices are mutually interconnected (Cassell et al., 1986; Gabbott et al., 2005; Vertes, 2004), whereas the basomedial nucleus of the amygdala (BMA) is reciprocally connected with the ventral part of the mPFC (vmPFC), including the infralimbic cortex (Hurley et al., 1991; Petrovich et al., 1996). The former functional unit has been shown to play a role in regulating high fear state and the related memory formation/storage (Kim et al., 2016a; Maren et al., 1996; Sierra-Mercado et al., 2011; Tye et al., 2011), while the latter one controls low fear state and is involved in extinction learning (Adhikari et al., 2015).

As a general principle, cortical function is efficiently and rapidly affected by subcortical inputs in a brain state-dependent manner. One of the subcortical afferent systems contributing critically to cortical network operation originates from the basal forebrain (BF) (Hasselmo & Sarter, 2011; Mesulam et al., 1983; Solari & Hangya, 2018; Zaborszky, 2002). In this brain region, three neuron types: cholinergic, GABAergic and glutamatergic cells are known to project to cortical areas (Farr et al., 1999; Goldbach et al., 1998; Henny & Jones, 2008; Pascual et al.,

2004). Recent studies have established that GABA is often a co-transmitter molecule in cholinergic cells, giving rise to complex responses in their postsynaptic neurons (Saunders et al., 2015; Takács et al., 2018). Interestingly, cholinergic cells from a given part of the BF have been proposed to target simultaneously such cortical areas that are functionally interconnected with each other (Gombkoto et al., 2021; Zaborszky et al., 2015). These results imply that BF cholinergic inputs may orchestrate activity in functionally related cortical areas, promoting interaction between regions and ultimately, enhancing the neural computation. However, this attractive hypothesis has not been fully verified.

The BF is a heterogeneous structure located in the medial-ventral part of the brain. Previous studies have revealed that the amygdala and mPFC receive cholinergic inputs primarily from the two main parts of the BF, horizontal limb of the diagonal band (HDB) and ventral pallidum/ substantia innominata (VP/SI) (Bloem et al., 2014; Mayo et al., 1984; Nagai et al., 1982). Whether the BA-dmPFC and the BMA-vmPFC networks can be simultaneously or differentially regulated by cholinergic afferents conveying salient information has yet to be determined. It is a particularly important question as several studies have shown a role of cholinergic system in fear related processes (Crimmins et al., 2023; Jiang et al., 2016; Knox, 2016; Mineur et al., 2022; Power et al., 2003).

In this study we aimed to reveal the structural basis of BF cholinergic control over the interconnected amygdala-mPFC fear circuits. We used tracing techniques and immunocytochemistry to map the location of cholinergic neurons along the BF innervating different parts of the amygdala and mPFC. We found that cholinergic neurons in the VP/SI target preferentially the BA and dmPFC. In contrast, HDB cholinergic cells innervate predominantly amygdala regions surrounding the BMA and vmPFC. Importantly, amygdala and mPFC projecting cholinergic neurons are intermingled, yet they form largely separate populations, but a group of cholinergic cells projects simultaneously to the amygdala and mPFC. Moreover, we found that VGLUT3 is present in VP/SI cholinergic somata and axon terminals located in the BA. On the other hand, we show that VGAT might be expressed in cholinergic neurons in the VP/SI and HDB transiently during development, but not in adulthood.

MATERIALS AND METHODS

Animals. In this study, C57Bl6 wild type mice, ChAT-Cre (www.jax.org, #006410), VGAT-IRES-Cre (www.jax.org, # 016962) and offspring of VGAT-IRES-Cre crossed with Ai6 reporter mouse line (CAG-LSL-ZsGreen1, www.jax.org, # 007906) and of VGLUT3-Cre (www.jax.org, #028534) crossed with Ai14 reporter mouse line (CAG-LSL-tdTomato, www.jax.or, #007914) were used. All experiments were performed in male and female mice 5-16 weeks of age. All effort was taken to minimize animal suffering and the number of animals used.

Retrograde tracing. Wild type mice were anaesthetized with 125 mg/kg ketamine and 5 mg/kg xylazine and mounted to a stereotaxic frame. Eyes were coated with corneal gel (Recugel Ophthalmic Gel), and body temperature was maintained with small animal heating pads (Supertech Instruments). The skin was removed from the skull, so the cranial sutures were clearly visible. The mouse head was set horizontally based on the level of the bregma and lambda. Anterior-posterior and medio-lateral coordinates were measured from the bregma. The skull was carefully drilled with a dental bur (Foredom), then dorso-ventral coordinates were measured from the level of the dura mater. To label BF neurons projecting to the amygdala region, we used Cholera Toxin B (CTB, 0.5 mg/99.5 µl distilled water, List Biological Laboratories) or FastBlue (FB, 5% in in 0.9% saline, Polysciences), which was iontophoretically injected (2/2 s on/off duty cycle, 2 µA pulses, for 5 min for CTB, 2/2 s on/off duty cycle, 5 µA pulses, for 7-10 min for FB) into the lateral amygdala (AP/ML/DV coordinates, -1.7/3.4/3.6 mm), BA (AP/ML/DV coordinates, -1.5/3.2/4.2 mm) or BMA (AP/ML/DV coordinates, -1.7/2.8/4.6 mm) unilaterally using a Drummond Recording Nanoject II (Drummond Scientific). To label BF neurons projecting to the mPFC, Fluoro-Gold (FG, 2% in 0.9% saline, Fluorochrome) or CTB was injected iontophoretically (for both tracers, 2/2 s on/off duty cycle, 2 µA pulses, for 5 min) into the prelimbic cortex (AP/ML/DV coordinates, 1.9/0.3/1.1-1.5 mm) and infralimbic cortex (AP/ML/DV coordinates, 1.9/0.3/1.9-2.2 mm). These retrograde tracers were applied to the brain through a glass pipette (ID = 0.530 mm ± 25 µm, OD 1.14 mm, World Precision Instruments) which was filled first with 50% glycerol (tap water: glycerol, 1:1) and then by the tracer. After 3-5 days following the injections, animals were anesthetized again with ketamine/xylazine mixture as above and perfused under deep anesthesia first with saline (0.9%) and then with 4% paraformaldehyde dissolved in 0.1 M phosphate buffer (PB, pH: 7.4, 100

mL/animal, Sigma-Aldrich). Brains were then removed and cut into 50-80 µm-thick coronal sections with a VT1000S Vibratome (Leica).

Anterograde tracing. To analyze the axonal arborization of BF cholinergic neurons projecting to the amygdala region and mPFC, we injected 30 nl of AAV8.CAG.GFP.FLEX (UNC Boyden, Lot# AV4910b) into the HDB (AP/ML/DV coordinates, 0.5/0.7/5.0 mm) or VP/SI (AP/ML/DV coordinates, 0.5/1.5/4.4 mm) in ChAT-Cre mice. The viruses were injected with a Nanoject III Programmable Nanoliter Injector (Drummond Scientific Company). During this surgery the same glass pipette was used as in retrograde tracing, but instead of glycerol, mineral oil (Sigma-Aldrich) was filled in the pipette first, then the virus. Injection speed was set to 3 nl/s until a clear change in the meniscus (mineral oil – virus border) was observed, then speed was set to 1 nl/s. After 4-5 weeks following the surgery, animals were anaesthetized and perfused the same way as described for retrograde tracing.

Retrograde-anterograde viral tracing. To investigate the dual projection of individual cholinergic cells from the basal forebrain (BF) to both the basolateral amygdala complex (BLA) and mPFC, we injected 3x100 nl AAV5.Ef1a.DIO.eYFP (Penn Core, Addgene: 27056) into the mPFC (AP/ML/DV coordinates 2.2, 1.9, 1.5/0.3/0.8 mm) or 2x100 nl AAV5.Ef1a.DIO.eYFP into the BLA (AP/ML/DV coordinates -2.0, -1.5/3.1/4.25 mm) unilaterally in ChAT-Cre mice. The injection method and parameters were consistent with those used in anterograde tracing. This approach allowed the cholinergic axon terminals from the BF, containing the Cre enzyme, to uptake the virus and express eYFP in their cell bodies retrogradely and visualize their axon collaterals. Subsequently, within 6-8 weeks following the injection, the expressed eYFP labeled the processes of cholinergic neurons including their remote axons, enabling the examination of the presence of axon collaterals within the amygdala region innervated by mPFC projecting cholinergic cells and vice versa. Following tissue processing, we compared the normalized axonal fluorescent intensity (utilizing NIS elements AR 5.3) obtained by retrograde-anterograde viral tracing and anterograde viral tracing (HDB, VP/SI) within the BLA and mPFC.

Immunostaining. After sectioning, fixed brain sections were washed 3 times for 10 minutes in 0.1M PB, then a blocking solution (10% NDS, Normal Donkey Serum, 0.5% Triton-x 100, 0.1M

PB) was applied for 30 minutes. The sections were incubated in a solution containing primary antibodies in addition to 2% NDS, 0.5% Triton-x 100 and 0.1M sodium azide dissolved in 0.1M PB for 1 day at room temperature, followed by 2 hours of incubation in the secondary antibody containing solution (1% NDS, 0.1M PB). Guinea pig anti-FG primary antibody (1:5000, Protos Biotech) and Alexa 488- or Cy3-conjugated donkey anti-guinea pig (1:500, Jackson ImmunoResearch) or goat anti-CTB primary antibody (1:20,000, List Biological Laboratory) and Cy3-conjugated donkey anti-goat (1:500, Jackson ImmunoResearch) were used to visualize FG- or CTB-containing BF neurons. Retrograde tracer Fast Blue, however, required no additional immunostaining. Rabbit anti-ChAT primary antibody (1:5000, SYSY) and Alexa 647- or Cy3-donkey anti-rabbit (1:500, Jackson ImmunoResearch) secondary antibody was used for visualizing ChAT+ neurons. Goat anti-GFP primary antibody (1:1000, Frontier Institute Co. Ltd) and Alexa 488-conjugated donkey anti-goat (1:500, Jackson ImmunoResearch) were used to enhance the visualization of axons in experiments using viral tracing.

To identify the neurochemical content of axon terminals in the amygdala, rabbit anti-ChAT (1:5000, SYSY) and rabbit anti- VAChT (vesicular acetylcholine transporter) primary antibody (1:1000, Frontier Institute Co. Ltd) and A488-conjugated donkey anti-rabbit (1:500, Jackson ImmunoResearch), goat anti-VGLUT3 (vesicular glutamate transporter type 3) primary antibody (1:1000, Frontier Institute Co. Ltd) and Cy3-conjugated donkey anti-goat (1:500, Jackson), guinea-pig anti- VGAT (vesicular GABA transporter) primary antibody (1:1000, Frontier Institute Co. Ltd) and Cy5-conjugated donkey anti-guinea pig (1:500, Jackson) were used. After the incubations, the sections were rinsed in 0.1M PB, mounted on slides in Vectashield (Vector Laboratories).

Confocal microscopy. Multicolor large images from different brain regions were taken with a C2 confocal laser scanning microscope (Nikon Europe, Amsterdam, The Netherlands) using a 10x (Plan Fluor 10x, N.A. 0.3, xy: 1.25 μm/pixel) and 20x objective (CFI Super Plan Fluor 20X, N.A. 0.45, xy: 0.58 μm/pixel). Multichannel images at a high resolution were acquired in channel series mode. This way quantitative analysis and localization maps of retrogradely labeled BF cells could be performed on the same images. To quantify the cholinergic and GABAergic content of retrogradely labeled BF neurons, the NIS-Elements software was used. Then, large images were exported to Neurolucida software (10.53 software, MBF Bioscience),

where the position of retrogradely labeled neurons as well as the brain structures and landmarks (ventral border of the slice, anterior commissure, midline) were indicated. This process was repeated at 3-3 coronal planes of the BF (0.62, 0.14, -0.34 mm from bregma) in all injected animals. The drawings from the corresponding coronal planes were precisely aligned and mapped onto the appropriate coronal section taken from the mouse brain atlas (Paxinos et al., 2004) using Adobe Photoshop (version 3.0, Adobe Inc.).

To reveal the neurochemical content of axon terminals in the amygdala region, confocal images were taken from each nucleus/subnucleus using a C2 microscope with a 60x objective (CFI Plan Apo VC60X Oil objective, N.A. 1.40; z (n=50) step size: 0.13 μm, xy: 0.08 μm/pixel). High resolution fluorescent images (2048x2048 pixel) from the injection sites in the HDB and VP/SI as well as amygdala region were taken using a 4x objective (C2 confocal laser scanning microscope, Plan Fluor 4x, N.A 0.13, xy: 1.54 μm/pixel). To quantify the VGAT content of BF cholinergic neurons, images were acquired in the HDB and VP/SI with a C2 confocal laser scanning microscope using a 10x objective (Plan Fluor 10x, N.A. 0.3, z (n=10) step size: 25.88 μm, xy: 1.25 μm/pixel).

Axon arborization maps. To determine the proportion of the labeled axons in each amygdala region and prefrontal cortical area, we imported the confocal images into Adobe Photoshop and quantified the pixels representing axons and compared to the total axonal arborization within the amygdala or prefrontal cortical region. To determine the borders of the amygdala areas based on the soma distributions, we mapped the amygdala region at the coronal planes using NeuN staining (1:1000, Milipore). In the case of the prefrontal cortex, we used the borders from the mouse brain atlas (Paxinos et al., 2004). Data are presented as mean ± SD.

RESULTS

Localization of amygdala-projecting cholinergic neurons in the BF

To reveal the sources of cholinergic innervation invading the amygdalar region from the BF, retrograde tracer Cholera Toxin B (CTB) was injected into the three distinct nuclei of the basolateral amygdala complex (BLA): lateral amygdala (LA, Fig. 1A1, (n=2)), basal amygdala (BA, Fig. 1A2, (n=4)) and basomedial amygdala (BMA, Fig. 1A3, (n=2)). In coronal sections obtained from these injected mice, we determined the location of the somata of amygdala-projecting neurons in the BF (Fig. 1B1). We found that BA-projecting BF neurons were located primarily in the VP/SI region (defined based on the (Paxinos et al., 2004)). In contrast, BMA-projecting BF neurons were found dominantly in the HDB (but also partially in the lateral preoptic area (LPO), median preoptic nucleus (MnPO), medial preoptic area (MPA)), forming a separate neuronal population with minimal overlap with BA-projecting BF neurons (Fig. 1C1-C3). Retrograde tracer injected to the LA, however, resulted in only a few labeled neurons that were in the HDB (Fig. 1C1). Next, we evaluated the cholinergic content of the amygdala-projecting BF neurons. After performing immunostaining against choline acetyltransferase (ChAT), we found that more than 60% of BA-projecting BF neurons were cholinergic (Fig. 1B1, B2, 130/212; n= 4 mice), while this ratio was around 25% (24/91; n= 2 mice) among BMA-projecting BF neurons. Altogether, these results show that the BF provides a prominent cholinergic innervation within the amygdala. Furthermore, neurons in the VP/SI preferentially innervate the BA, while those neurons located in the HDB project predominantly to the BMA and to a lesser extent to the LA. The difference in the ratio of BF cholinergic neurons innervating the distinct amygdalar nuclei is in accord with earlier observations, showing more profound presence of cholinergic fibers in the BA in comparison with the surrounding areas (Mesulam et al., 1983; Nagai et al., 1982; Vereczki et al., 2021; Wilson & Fadel, 2017).

Non-overlapping cholinergic projections within the amygdalar region originate from distinct BF areas

To confirm that cholinergic neurons in the separate BF regions innervate different amygdalar nuclei, we injected a small amount (30 nl) of AAV8.CAG.Flex.GFP into the HDB (Fig. 2A) and VP/SI (Fig. 2D) of ChAT-Cre mice, respectively. This approach enabled us to visualize the cholinergic axonal projections of BF neurons innervating the amygdalar region. In line with our

retrograde tracing data, we observed that ChAT+ neurons in the HDB projected mostly to the BMA and other surrounding areas, such as the centromedial amygdaloid nucleus (CeM), medial amygdaloid nucleus (MeA), anterior cortical amygdaloid nucleus (ACo), dorsal endopiriform nucleus (DEn), piriform cortex (Pir), but largely avoiding the BA (Fig. 2B, C, G). Although there were some labeled axons in the LA, this connection appeared to be weak compared to other neighboring fields, an observation, which is in accord with the small number of HDB neurons labeled retrogradely from the LA. On the other hand, ChAT+ neurons in the VP/SI almost exclusively innervated the BA, with marginal projections into the medial part of the central nucleus, BMA and piriform cortex (Fig. 2E-G). These results show that cholinergic fibers from the HDB and VP/SI parcel the amygdalar region in a mutually exclusive manner.

Sources of cholinergic afferents to the BLA and mPFC

Previous studies uncovered that the mPFC and BLA are reciprocally interconnected cortical regions playing a role in similar cognitive processes (Arruda-Carvalho & Clem, 2015; Burgos-Robles et al., 2009; Herry et al., 2008; Little & Carter, 2013; Sotres-Bayon et al., 2012; Weiskrantz, 1956). These earlier observations raised the question of whether the same or different ChAT+ neuronal populations provide cholinergic control for these two mutually interconnected areas. Therefore, we analyzed the cholinergic projections from the HDB and VP/SI towards the mPFC in the same mice as we did for the innervation of the amygdalar region (Fig. 3). We found that both BF areas projected to the mPFC, namely the anterior cingulate (ACC), prelimbic (PL) and infralimbic (IL) cortices. While the HDB tended to project to the ventral part of the mPFC (medial orbital cortex (MO), IL, dorsal peduncular cortex (DP), cingulate cortex, area 2 (Cg2)) (Fig. 3A, B, E), the VP/SI innervated its dorsal part (secondary motor cortex (M2), cingulate cortex, area 1 (Cg1) and PL)(Fig. 3C-E). The most conspicuous differences were found at the level of 2.4 mm from the bregma, where the HDB predominantly innervated the MO, while the VP/SI had prominent projections to the PL, Cg1 and M2 (Fig. 3B, D). At the bregma level of 1.1 mm, there was a similar exclusive projection pattern: cholinergic cells in the HDB innervated the Cg1, but not the M2, while cholinergic cells in the VP/SI gave rise to projections to the M2, but not to the Cg2 (Fig. 3B, D). Altogether, these results show that cholinergic innervation originated from the HDB and VP/SI terminates in the differential parts of the mPFC and amygdalar regions. Namely, ChAT+ neurons in the HDB send axons to the

ventral-medial part of the PFC and to the most amygdalar areas, apart from the BA, while ChAT+ neurons in the VP/SI prefer to terminate in the dorso-medial part of the PFC and BA.

The next question we asked was whether the same BF neurons send axonal collaterals into both the mPFC and amygdalar regions, or separate populations of neurons innervate these two brain structures. To reveal the logic underlying the cholinergic control of the mPFC and amygdala, we performed retrograde-anterograde viral tracing in ChAT-Cre mice by injecting AAV5.Ef1a.DIO.eYFP into the mPFC or BLA in separate animals (Fig. 4). This approach allows us to reveal whether neurons projecting to a given area have axonal collaterals in the brain regions of interest. Thus, AAV injection into the BLA may visualize axons in the mPFC if a portion of BF cholinergic neurons simultaneously project to BLA and mPFC (Fig. 4C1) and vice versa, mPFC injection should result in axonal labeling in the BLA (Fig. 4C4). Our retrograde-anterograde viral tracing confirmed that there are ChAT+ neurons in the BF that send axons both to the mPFC and BLA (Fig. $4C_1$, C_4, D). To compare the axon density between experiments obtained by retrograde-anterograde vs anterograde labeling, we determined the normalized fluorescent intensity of axon labeling in the mPFC and BLA (PL/Cg1, BA, IL, BMA) (Fig 4C vs A, B). We observed that retrograde-anterograde viral tracing produced substantially less, but visible axonal labeling in the target regions in comparison to anterograde viral tracing. These results suggest that the mPFC-BLA circuit receives dual cholinergic control: there are ChAT+ neurons that project either to the BLA or mPFC, whereas there is a group of ChAT+ neurons that send collaterals to both cortical structures.

VGLUT3 content typifies cholinergic neurons projecting to the BA

A previous study obtained in rats uncovered (Poulin et al., 2006) that BF cholinergic neurons projecting to the amygdala express vesicular glutamate transporter type 3 (VGLUT3). To clarify whether amygdala-projecting cholinergic neurons also contain VGLUT3 in mice, we revealed the neurons with VGLUT3 content genetically by crossing VGLUT3-Cre and Ai14 reporter mice. In offspring we performed immunostaining against ChAT that allowed us to quantify the number of cholinergic neurons in the HDB and VP/SI that expressed VGLUT3, too. We observed that 71.19% (168/236, n=2) of cholinergic neurons in the VP/SI expressed VGLUT3, whereas this ratio was 33.69% (94/279, n=2) in the HDB. These data predict that most cholinergic axon terminals within the BA should also contain VGLUT3 immunolabeling,

whereas the ratio of the double labeled boutons for ChAT/VAChT and VGLUT3 should be substantially less in other amygdalar areas. In agreement with this prediction, we found that, among all amygdalar areas, the BA had the highest ratio of axon terminals immunostained for both ChAT/VAChT and VGLUT3 (Fig. 5A). Interestingly, this ratio was not homogeneous within this nucleus: its anterior part (63.28%± 8.58, 324/512, n=3) contained twice as many double immunopositive axonal boutons than its posterior part (Fig. 5D, 29.67%± 3.51, 89/300, n=3). As expected, in neighboring regions, the co-expression of ChAT/VAChT and VGLUT3 was minimal (Fig. 5B, D). These results together suggest that cholinergic pathway from the VP/SI that terminates in the BA contains typically VGLUT3, while cholinergic fibers located in other amygdalar regions that originates from the HDB express this glutamate transporter at a much lower frequency. In addition, these observations further strengthen the conclusion that the BLA receives cholinergic control from two distinct BF sources that differ in their VGLUT3 content.

GABAergic phenotype is not characteristic for cholinergic neurons in the HDB and VP/SI in adult mice

Previous studies convincingly demonstrated that GABA can be released from cholinergic axon terminals in the neocortex (Saunders et al., 2015), hippocampus (Takács et al., 2018) and striatum (Lozovaya et al., 2018). To assess whether cholinergic neurons in the HDB and VP/SI are also GABAergic, we visualized inhibitory cells in the BF by crossing VGAT-Cre with Ai9 reporter mice (CAG-LSL- ZsGreen1, Fig. 6A1, B1), whereas ChAT content of neurons was revealed by immunostaining (Fig. 6A2, B2). We found that 96.98% (546/563, n=3) of cholinergic neurons expressed the reporter protein under the control of VGAT promoter in the HDB, whereas this ratio was 58.8% (137/233, n=3) in the VP/SI (Fig. 6E, dark green). To confirm the GABAergic nature of cholinergic afferents in the BLA, we examined the VGAT immunoreactivity in cholinergic axon terminals in wild type mice. To our surprise, we observed no co-expression of VGAT and cholinergic markers (ChAT and VAChT)(Fig. 5C, 0.75%, 3/400, n=2) in axonal boutons at the amygdala level. To resolve this contradiction, we labeled BF GABAergic cells in adult VGAT-Cre mice by injecting AAV8.CAG.Flex.GFP virus simultaneously into the HDB and VP/SI (Fig. 6C1, D1). After 4 weeks following the injections, we performed immunostaining against ChAT (Fig. 6C2, D2) and counted the GFP content of

cholinergic cells in the BF (Fig. 6C3, D3). Under these circumstances, we found that there were only a few neurons co-expressing ChAT and GFP both in the HDB (3.06%, 19/620, n=3) and VP/SI (1.19%, 3/253, n=3) (Fig. 6E light green). These data are in line with the findings that cholinergic axon terminals in the amygdala infrequently contain VGAT immunoreactivity in adulthood (Fig. 5C). Thus, our results collectively show that in adult mice, GABA is below the detectability threshold in cholinergic neurons in the HDB and VP/SI. However, these BF neurons may transiently express GABA during the development as indicated by the experiments obtained in offspring of VGAT-Cre and Ai9 mice.

DISCUSSION

In this study we have investigated the cholinergic innervation of the reciprocally interconnected mPFC- amygdala regions. Our main findings are the followings. 1) Cholinergic cells located in two separate BF nuclei, in the HDB and VP/SI innervate different parts of the BLA in a mutually exclusive manner, while they also project to different parts of the mPFC through the dorso-ventral axis. 2) Using retrograde-anterograde viral tracing we provide evidence that a cholinergic cell group simultaneously innervates the BLA and mPFC. 3) Most cholinergic cells in the VP/SI that project to the BA co-express VGLUT3, while the presence of VGLUT3 is much less typical for cholinergic cells and their axon terminals in the HDB and other amygdala areas, respectively. 4) VGAT in amygdala-projecting cholinergic cells may be expressed during development, but not in adulthood.

Our results are overall in a good agreement with previous observations showing that the majority of BF neurons (61%) located in the VP/SI innervating the BA express ChAT (Poulin et al., 2006). In addition, we provide evidence that the HDB innervates the BMA, yet the ratio of cholinergic neurons in this pathway is considerably lower (25%). The difference in the proportion of cholinergic neurons within the BF innervation that terminates in the BA and BMA is also reflected in the abundance of cholinergic fibers in these amygdala nuclei (Fig. 5E1).

In our study we found striking similarities in the distribution of BF afferents innervating the mPFC to that observed earlier (Bloem et al., 2014). However, we substantially expanded these previous findings by showing that the same BF regions distinctly projected to the amygdala region. Here, we show that, besides the extensively studied nucleus basalis of Meynert (Crouse

et al., 2020; Jiang et al., 2016; Kitt et al., 1987; Mallet et al., 1995), the VP/SI gives rise to a significant innervation to the BA, while the HDB provides inputs to additional amygdala areas albeit less intensively. We also observed a cholinergic projection from the VP/SI to the CeM, in agreements with a recent study (Aitta-aho et al., 2018). Based on our tracing experiments, two parallel cholinergic innervation patterns can be outlined: 1) the VP/SI to dmPFC and BA and 2) the HDB to vmPFC and LA/BMA projections. These parallel pathways might be important in transmitting salient information into the amygdala and mPFC controlling functions that are related to fear- and reward coding, social memory and interaction (Jiang et al., 2016; Kim et al., 2016; Lee & Kim, 2019; Okada et al., 2021; Robert et al., 2021). A recent study reported that the HDB is important in 1) predicting whether a perceptual outcome in a behavioral task was hit or miss and 2) encoding the omission of anticipated rewards, while the VP/SI can encode 1) nociceptive inputs and auditory stimuli and 2) learning related plasticity of auditory cues associated with punishment (Robert et al., 2021). These observations highlight the distinct functions for the two parallel cholinergic pathways.

To explore the structure of cholinergic control from these BF regions we used double retrograde tracing. The drawback of this method is that if we inject small amount of tracer into brain areas, which has extensive rostro-caudal spread – such as the mPFC and amygdala – we might not have an overlap in the retrogradely labeled cells within the BF, therefore, we can miss those cholinergic cells who project to both areas. Meanwhile, larger injections have the risk to spread through region borders, resulting in unspecific labeling. To overcome this issue, we made multiple small injections within the mPFC and BLA along the anterior-posterior axis, and in the dmPFC at 2 dorso-ventral coordinates. Based on these experiments, we found that a small percentage of cholinergic cells projects to both mPFC and BLA. To confirm or reject the hypothesis that there are cholinergic neurons with dual projection, we used retrograde-anterograde viral tracing. We found that indeed there are cholinergic neurons in the HDB and VP/SI, which innervate both the mPFC and the BLA region at the same time. This is in line with previous study (Li et al., 2017), where the authors show that single cholinergic cells in the BF projected to multiple cortical areas – the isocortex, olfactory bulb, hippocampus – simultaneously. Altogether, these findings show that cholinergic cells in the HDB and VP/SI predominantly provide separate innervation to the amygdala and mPFC, but a group of cells

innervate both regions at the same time, an innervation strategy, which allows for simultaneous as well as independent control of operation in these cortical areas.

A portion of subcortical neuromodulatory afferents typically express more than one kind of neurotransmitter molecule. For instance, dopaminergic cells can release GABA or glutamate in addition to dopamine (Stuber et al., 2010; Tecuapetla et al., 2010; Tritsch et al., 2012, 2014). Similarly, BF cholinergic cells projecting to the cortex and hippocampus often contain and release GABA (Saunders et al., 2015; Takács et al., 2018). Here, we showed that 70% of VP/SI cholinergic neurons co-express VGLUT3, while this ratio is ~30% in the HDB. Moreover, we found that 60% of cholinergic axon terminals in the BA contain VGLUT3. These results are in agreement with data obtained previously in rats (Poulin et al., 2006), showing that within the two parallel BF to mPFC and amygdala circuits, the VP/SI to BA connection contains significantly more VGLUT3, and therefore might release both glutamate and acetylcholine. In addition, we found that cholinergic cells in the HDB and VP/SI express GABA only transiently during development, but not in adulthood, unlike medial septal cholinergic neurons (Takács et al., 2018). Thus, GABA is present neither in the cholinergic somata, nor in cholinergic axon terminals within the BA in wild type mice or virally labeled neurons in adult VGAT-Cre mice, suggesting that GABA is not a co-transmitter molecule in the BF-amygdala pathway in adult mice.

Our results indicate that there are two parallel cholinergic circuits that are in the position to control opposing fear conditions: 1) during high fear state the VP/SI may regulate the dmPFC-BA circuits, while 2) during low fear state the HDB may support the vmPFC-BMA network operation. Based on our findings, the HDB and VP/SI innervate these interconnected regions of the amygdala and mPFC mostly independently, but we identified a cholinergic cell group that simultaneously innervates both regions. This organization of cholinergic projections allows for simultaneous as well as independent control of targeted cortical areas, maximizing computational support for their coordinated functioning. The uncovered structural arrangement sheds light on logic underlying cholinergic control of cortical function and has implications for understanding the neural basis of emotional regulation.

REFERENCES

Adhikari, A., Lerner, T. N., Finkelstein, J., Pak, S., Jennings, J. H., Davidson, T. J., Ferenczi, E., Gunaydin, L. A., Mirzabekov, J. J., Ye, L., Kim, S. Y., Lei, A., & Deisseroth, K. (2015). Basomedial amygdala mediates top-down control of anxiety and fear. *Nature*, *527*(7577), 179–185. https://doi.org/10.1038/nature15698

Aitta-aho, T., Hay, Y. A., Phillips, B. U., Saksida, L. M., Bussey, T. J., Paulsen, O., & Apergis-Schoute, J. (2018). Basal Forebrain and Brainstem Cholinergic Neurons Differentially Impact Amygdala Circuits and Learning-Related Behavior. *Current Biology*, *28*(16), 2557-2569.e4. https://doi.org/10.1016/j.cub.2018.06.064

Bloem, B., Schoppink, L., Rotaru, D. C., Faiz, A., Hendriks, P., Mansvelder, H. D., van de Berg, W. D. J., & Wouterlood, F. G. (2014). Topographic mapping between basal forebrain cholinergic neurons and the medial prefrontal cortex in mice. *Journal of Neuroscience*, *34*(49), 16234–16246. https://doi.org/10.1523/JNEUROSCI.3011-14.2014

Burgos-Robles, A., Vidal-Gonzalez, I., & Quirk, G. J. (2009). Sustained conditioned responses in prelimbic prefrontal neurons are correlated with fear expression and extinction failure. *Journal of Neuroscience*, *29*(26), 8474–8482. https://doi.org/10.1523/JNEUROSCI.0378-09.2009

Cassell, M. D., Wright, D. J., & WRIGHT Topography, D. J. (1986). Topography of Projections From the Medial Pretiontal Cortex to the Amygdala in the Rat. In *Brain Research Bulletin* (Vol. 17). Ankho International Inc.

Crimmins, B. E., Lingawi, N. W., Chieng, B. C., Leung, B. K., Maren, S., & Laurent, V. (2023). Basal forebrain cholinergic signaling in the basolateral amygdala promotes strength and durability of fear memories. *Neuropsychopharmacology*, *48*(4), 605–614. https://doi.org/10.1038/s41386-022-01427-w

Crouse, R. B., Kim, K., Batchelor, H. M., Girardi, E. M., Kamaletdinova, R., Chan, J., Rajebhosale, P., Pittenger, S. T., Role, L. W., Talmage, D. A., Jing, M., Li, Y., Gao, X. B., Mineur, Y. S., & Picciotto, M. R. (2020). Acetylcholine is released in the basolateral amygdala in response to predictors of reward and enhances the learning of cue-reward contingency. *ELife*, *9*, 1–31. https://doi.org/10.7554/ELIFE.57335

Davis M. Neurobiology of fear responses: the role of the amygdala. J Neuropsychiatry Clin Neurosci. 1997 Summer;9(3):382-402. doi: 10.1176/jnp.9.3.382. PMID: 9276841.

Farr, S. A., Uezu, K., Flood, J. F., & Morley, J. E. (1999). Septo-hippocampal drug interactions in post-trial memory processing. In *Brain Research* (Vol. 847). www.elsevier.comrlocaterbres

Gabbott, P. L. A., Warner, T. A., Jays, P. R. L., Salway, P., & Busby, S. J. (2005). Prefrontal cortex in the rat: Projections to subcortical autonomic, motor, and limbic centers. *Journal of Comparative Neurology*, *492*(2), 145–177. https://doi.org/10.1002/cne.20738

Goldbach, R., Allgaier, C., Heimrich, B., & Jackisch, R. (1998). Postnatal development of muscarinic autoreceptors modulating acetylcholine release in the septohippocampal cholinergic system I. Axon terminal region: hippocampus. In *Developmental Brain Research* (Vol. 108). https://doi: 10.1016/s0165-3806(98)00026-1.

Gombkoto, P., Gielow, M., Varsanyi, P., Chavez, C., & Zaborszky, L. (2021). Contribution of the basal forebrain to corticocortical network interactions. *Brain Structure and Function*, *226*(6), 1803–1821. https://doi.org/10.1007/s00429-021-02290-z

Hasselmo, M. E., & Sarter, M. (2011). Modes and models of forebrain cholinergic neuromodulation of cognition. In *Neuropsychopharmacology* (Vol. 36, Issue 1, pp. 52–73). https://doi.org/10.1038/npp.2010.104

Henny, P., & Jones, B. E. (2008). Projections from basal forebrain to prefrontal cortex comprise cholinergic, GABAergic and glutamatergic inputs to pyramidal cells or interneurons. *European Journal of Neuroscience*, *27*(3), 654–670. https://doi.org/10.1111/j.1460-9568.2008.06029.x

Herry, C., Ciocchi, S., Senn, V., Demmou, L., Müller, C., & Lüthi, A. (2008). Switching on and off fear by distinct neuronal circuits. *Nature*, *454*(7204), 600–606. https://doi.org/10.1038/nature07166

Hurley, K. M., Herbert, H., Moga, M. M., & Saper, C. B. (1991). Efferent projections of the infralimbic cortex of the rat. *Journal of Comparative Neurology*, *308*(2), 249–276. https://doi.org/10.1002/cne.903080210

Izquierdo, I., Furini, C. R. G., & Myskiw, J. C. (2016). Fear memory. *Physiol Rev*, *96*, 695–750. https://doi.org/10.1152/physrev.00018.2015.-Fear

Jiang, L., Kundu, S., Lederman, J. D. D., López-Hernández, G. Y. Y., Ballinger, E. C. C., Wang, S., Talmage, D. A. A., & Role, L. W. W. (2016). Cholinergic Signaling Controls Conditioned Fear Behaviors and Enhances Plasticity of Cortical-Amygdala Circuits. *Neuron*, *90*(5), 1057–1070. https://doi.org/10.1016/j.neuron.2016.04.028

Kim, J., Pignatelli, M., Xu, S., Itohara, S., & Tonegawa, S. (2016). Antagonistic negative and positive neurons of the basolateral amygdala. *Nature Neuroscience*, *19*(12), 1636–1646. https://doi.org/10.1038/nn.4414

Kitt, C. A., Mitchell, S. J., Delong, M. R., Wainer, B. H., & Price, D. L. (1987). Fiber pathways of basal forebrain cholinergic neurons in monkeys. In *Brain Research* (Vol. 406, Issue 16). https://doi: 10.1016/0006-8993(87)90783-9.

Knox, D. (2016). The role of basal forebrain cholinergic neurons in fear and extinction memory. In *Neurobiology of Learning and Memory* (Vol. 133, pp. 39–52). Academic Press Inc. https://doi.org/10.1016/j.nlm.2016.06.001

Lacroix, L., Spinelli, S., Heidbreder, C. A., & Feldon, J. (2000). Differential Role of the Medial and Lateral Prefrontal Cortices in Fear and Anxiety. *Behavioral Neuroscience*, *114*(6), 1119–1130. https://doi.org/10.1037/0735-7044.114.6,1119

LeDoux JE. (2000). Emotion circuits in the brain. Annu Rev Neurosci. 2000; 23:155-84. https://doi: 10.1146/annurev.neuro.23.1.155.

Lee, S., & Kim, J. H. (2019). Basal forebrain cholinergic-induced activation of cholecystokinin inhibitory neurons in the basolateral amygdala. *Experimental Neurobiology*, *28*(3), 320–328. https://doi.org/10.5607/en.2019.28.3.320

Li, X., Yu, B., Sun, Q., Zhang, Y., Ren, M., Zhang, X., Li, A., Yuan, J., Madisen, L., Luo, Q., Zeng, H., Gong, H., & Qiu, Z. (2017). Generation of a whole-brain atlas for the cholinergic system and mesoscopic projectome analysis of basal forebrain cholinergic neurons. *Proceedings of the National Academy of Sciences of the United States of America*, *115*(2), 415–420. https://doi.org/10.1073/pnas.1703601115

Little, J. P., & Carter, A. G. (2013). Synaptic mechanisms underlying strong reciprocal connectivity between the medial prefrontal cortex and basolateral amygdala. *Journal of Neuroscience*, *33*(39), 15333–15342. https://doi.org/10.1523/JNEUROSCI.2385-13.2013

Lozovaya, N., Eftekhari, S., Cloarec, R., Gouty-Colomer, L. A., Dufour, A., Riffault, B., Billon-Grand, M., Pons-Bennaceur, A., Oumar, N., Burnashev, N., Ben-Ari, Y., & Hammond, C. (2018). GABAergic inhibition in dual-transmission cholinergic and GABAergic striatal interneurons is abolished in Parkinson disease. *Nature Communications*, *9*(1). https://doi.org/10.1038/s41467-018-03802-y

Mallet, P. E., Beninger, R. J., Flesher, S. N., Jhamandas, -khem, & Roland Boegman, -and J. (1995). Nucleus Basalis Lesions: Implication of Basoamygdaloid Cholinergic Pathways in Memory. In *Brain Research Bulletin* (Vol. 36, Issue I). https://doi: 10.1016/0361-9230(94)00162-t.

Maren, S., Aharonov, G., Stote, D. L., & Fanselow, M. S. (1996). 7V-Methyl-D-Aspartate Receptors in the Basolateral Amygdala Are Required for Both Acquisition and Expression of Conditional Fear in Rats. In *Behavioral Neuroscience* (Vol. 110, Issue 6). https:// doi: 10.1037//0735-7044.110.6.1365.

Mayo, W., Dubois, B., Ploska, A., Javoy-Agid, F., Agid, Y., Le Moal, M., & Simon, H. (1984). Cortical cholinergic projections from the basal forebrain of the rat, with special reference to the prefrontal cortex innervation. In *Neuroscience Letters* (Vol. 47). https://doi: 10.1016/0304-3940(84)90421-x.

Mesulam, M. -Marsel, Mufson, E. J., Levey, A. I., & Wainer, B. H. (1983). Cholinergic innervation of cortex by the basal forebrain: Cytochemistry and cortical connections of the

septal area, diagonal band nuclei, nucleus basalis (Substantia innominata), and hypothalamus in the rhesus monkey. *Journal of Comparative Neurology*, *214*(2), 170–197. https://doi.org/10.1002/cne.902140206

Mineur, Y. S., Mose, T. N., Maibom, K. L., Pittenger, S. T., Soares, A. R., Wu, H., Taylor, S. R., Huang, Y., & Picciotto, M. R. (2022). ACh signaling modulates activity of the GABAergic signaling network in the basolateral amygdala and behavior in stress-relevant paradigms. *Molecular Psychiatry*, *27*(12), 4918–4927. https://doi.org/10.1038/s41380-022-01749-7

Nagai, T., Kimura, H., Maeda, T., Mcgeer, P. L., Peng, F., & Mcgeer2, E. G. (1982). Cholinergic projections from the basal forebrain of rat to the amygdala'. In *Society for Neuroscience Printed in U.S.A* (Vol. 2, Issue 4). https://doi: 10.1523/JNEUROSCI.02-04-00513.1982.

Okada, K., Nishizawa, K., Kobayashi, T., Sakata, S., Hashimoto, K., & Kobayashi, K. (2021). Different cholinergic cell groups in the basal forebrain regulate social interaction and social recognition memory. *Scientific Reports*, *11*(1). https://doi.org/10.1038/s41598-021-93045-7

Pascual, M., Pérez-Sust, P., & Soriano, E. (2004). The GABAergic septohippocampal pathway in control and reeler mice: Target specificity and termination onto reelin-expressing interneurons. *Molecular and Cellular Neuroscience*, *25*(4), 679–691. https://doi.org/10.1016/j.mcn.2003.12.009

Paxinos, G., Franklin, K. B. J., Paxinos, G and Franklin, K. B. J., Paxinos, G., & Franklin, K. B. J. (2004). Mouse Brain in Stereotaxic Coordinates. In *Academic Press* (Vol. 2nd). https://doi.org/10.1016/S0306-4530(03)00088-X

Petrovich, G. D., Risold, P. Y., & Swanson, L. W. (1996). Organization of projections from the basomedial nucleus of the amygdala: A PHAL study in the rat. *Journal of Comparative Neurology*, *374*(3), 387–420. https://doi.org/10.1002/(SICI)1096-9861(19961021)374:3<387::AID-CNE6>3.0.CO;2-Y

Poulin, A. N., Guerci, A., Mestikawy, S. El, & Semba, K. (2006). Vesicular Glutamate Transporter 3 Immunoreactivity Is Present in Cholinergic Basal Forebrain Neurons Projecting to the Basolateral Amygdala in Rat. *The Journal of Comparative Neurology*, *498*(5), 690–711. https://doi.org/10.1002/cne.21081

Power, A. E., Vazdarjanova, A., & McGaugh, J. L. (2003). Muscarinic cholinergic influences in memory consolidation. *Neurobiology of Learning and Memory*, *80*(3), 178–193. https://doi.org/10.1016/S1074-7427(03)00086-8

Robert, B., Kimchi, E. Y., Watanabe, Y., Chakoma, T., Jing, M., Li, Y., & Polley, D. B. (2021). A functional topography within the cholinergic basal forebrain for encoding sensory cues and behavioral reinforcement outcomes. *Elife*, *10:e69514*. https://doi.org/10.7554/eLife

Saunders, A., Granger, A. J., & Sabatini, B. L. (2015). Corelease of acetylcholine and GABA from cholinergic forebrain neurons. *Elife*, *4:e06412*. https://doi.org/10.7554/eLife.06412.001

Sierra-Mercado, D., Padilla-Coreano, N., & Quirk, G. J. (2011). Dissociable roles of prelimbic and infralimbic cortices, ventral hippocampus, and basolateral amygdala in the expression and extinction of conditioned fear. *Neuropsychopharmacology*, *36*(2), 529–538. https://doi.org/10.1038/npp.2010.184

Solari, N., & Hangya, B. (2018). Cholinergic modulation of spatial learning, memory and navigation. In *European Journal of Neuroscience* (Vol. 48, Issue 5, pp. 2199–2230). Blackwell Publishing Ltd. https://doi.org/10.1111/ejn.14089

Sotres-Bayon, F., Sierra-Mercado, D., Pardilla-Delgado, E., & Quirk, G. J. (2012). Gating of Fear in Prelimbic Cortex by Hippocampal and Amygdala Inputs. *Neuron*, *76*(4), 804–812. https://doi.org/10.1016/j.neuron.2012.09.028

Stuber, G. D., Hnasko, T. S., Britt, J. P., Edwards, R. H., & Bonci, A. (2010). Dopaminergic terminals in the nucleus accumbens but not the dorsal striatum corelease glutamate. *Journal of Neuroscience*, *30*(24), 8229–8233. https://doi.org/10.1523/JNEUROSCI.1754-10.2010

Takács, V. T., Cserép, C., Schlingloff, D., Pósfai, B., Szőnyi, A., Sos, K. E., Környei, Z., Dénes, Á., Gulyás, A. I., Freund, T. F., & Nyiri, G. (2018). Co-transmission of acetylcholine and GABA regulates hippocampal states. *Nature Communications*, *9*(1). https://doi.org/10.1038/s41467-018-05136-1

Tecuapetla, F., Patel, J. C., Xenias, H., English, D., Tadros, I., Shah, F., Berlin, J., Deisseroth, K., Rice, M. E., Tepper, J. M., & Koos, T. (2010). Glutamatergic signaling by mesolimbic dopamine neurons in the nucleus accumbens. *Journal of Neuroscience*, *30*(20), 7105–7110. https://doi.org/10.1523/JNEUROSCI.0265-10.2010

Tovote, P., Fadok, J. P., & Luthi, A. (2015). Neuronal circuits for fear and anxiety. *Nat Rev Neurosci*, *16*(6), 317–331. https://doi.org/10.1038/nrn3945

Tritsch, N. X., Ding, J. B., & Sabatini, B. L. (2012). Dopaminergic neurons inhibit striatal output through non-canonical release of GABA. *Nature*, *490*(7419), 262–266. https://doi.org/10.1038/nature11466

Tritsch, N. X., Oh, W. J., Gu, C., & Sabatini, B. L. (2014). Midbrain dopamine neurons sustain inhibitory transmission using plasma membrane uptake of GABA, not synthesis. *ELife*, *2014*(3). https://doi.org/10.7554/eLife.01936

Tye, K. M., Prakash, R., Kim, S. Y., Fenno, L. E., Grosenick, L., Zarabi, H., Thompson, K. R., Gradinaru, V., Ramakrishnan, C., & Deisseroth, K. (2011). Amygdala circuitry mediating reversible and bidirectional control of anxiety. *Nature*, *471*(7338), 358–362. https://doi.org/10.1038/nature09820

Vereczki, V. K., Müller, K., Krizsán, É., Máté, Z., Fekete, Z., Rovira-Esteban, L., Veres, J. M., Erdélyi, F., & Hájos, N. (2021). Total number and ratio of GABAergic neuron types in the mouse lateral and basal amygdala. *Journal of Neuroscience*, *41*(21), 4575–4595. https://doi.org/10.1523/JNEUROSCI.2700-20.2021

Vertes, R. P. (2004). Differential Projections of the Infralimbic and Prelimbic Cortex in the Rat. *Synapse*, *51*(1), 32–58. https://doi.org/10.1002/syn.10279

Weiskrantz L. (1956). Behavioral changes associated with ablation of the amygdaloid complex in monkeys. J Comp Physiol Psychol. Aug;49(4):381-91. https://doi: 10.1037/h0088009.

Wilson, M. A., & Fadel, J. R. (2017). Cholinergic regulation of fear learning and extinction. *Journal of Neuroscience Research*, *95*(3), 836–852. https://doi.org/10.1002/jnr.23840

Zaborszky, L. (2002). The modular organization of brain systems. Basal forebrain: the last frontier. *Progress in Brain Research*, *136*, 359–372. https://doi.org/10.1016/S0079-6123(02)36030-8

Zaborszky, L., Csordas, A., Mosca, K., Kim, J., Gielow, M. R., Vadasz, C., & Nadasdy, Z. (2015). Neurons in the basal forebrain project to the cortex in a complex topographic organization that reflects corticocortical connectivity patterns: An experimental study based on retrograde tracing and 3D reconstruction. *Cerebral Cortex*, *25*(1), 118–137. https://doi.org/10.1093/cercor/bht210

FIGURE LEGEDS

Fig. 1. Characterization of retrogradely labeled BLA-projecting BF neurons.

(A) Pseudo-colored images showing the injection sites of different BLA regions, (A1) Lateral Amygdala (LA), (A2) Basal Amygdala (BA), (A3) Basomedial Amygdala (BMA). Scale bar: 500 µm.

(B1) An example large image taken from the basal forebrain (bregma 0.62 mm, BF) showing BA-projecting BF cells in blue, and ChAT-immunoreactive cells in white. Scale bar: 500 µm.

(B2-3) Images taken from BF showing expression of ChAT (choline acetyltransferase, B3, white arrow) in BA-projecting BF cells (B2). Small blue arrows indicate ChAT-positive cells without tracer content. Scale bar: 50 µm.

(C1-3) Positions of retrogradely labeled BLA-projecting BF neurons in different coronal planes of the BF. 61±7.08% of BA-projecting BF cells express ChAT (130/212; n= 4 mice), while 26.37 ±7.71% of BMA-projecting BF cells express ChAT (24/91; n= 2 mice). Purple: LA-projecting cells, Blue: BA-projecting cells, Green: BMA-projecting cells. Aca, anterior commissure, anterior part; HDB, nucleus of the horizontal limb of the diagonal band; LPO, lateral preoptic area; MnPO, median preoptic nucleus; MS, medial septal nucleus; SI, substantia innominata; VP, ventral pallidum.

Fig. 2. Distribution of anterogradely labeled cholinergic projections in the amygdala region from the HDB and VP/SI.

(A) Example injection sites of 30 nl AAV8.CAG.flex.GFP injected to the HDB in ChAT-Cre mice. Scale bar: 500 µm.

(B) Coronal images taken at different amygdala planes showing cholinergic projections from the HDB. Scale bar: 500 µm.

(C) Overlaid representative cholinergic projections from the HDB. Axons visualized in different animals (n=3) are shown in different colors. Borders of distinct amygdala regions were drawn based on NeuN staining.

(D) Example injection sites of 30 nl AAV8.CAG.flex.GFP injected to the VP/SI in ChAT-Cre mice.

(E) Coronal images from different amygdala planes showing cholinergic projections from the VP/SI.
(F) Overlaid representative cholinergic projections from the VP/SI. Axons revealed in different animals (n=4) are shown in distinct colors. Borders of distinct amygdala regions are drawn based on NeuN staining.
(G) Percentage of amygdala region-projecting HDB and VP/SI cholinergic axons in each nucleus/region. ACo, anterior cortical amygdaloid nucleus; AHi, amygdalohippocampal area; APir, amygdalopiriform transition area; BA, basal amygdaloid nucleus; BAP, basal amygdaloid nucleus, posterior part; BMA, basomedial amygdaloid nucleus, anterior part; BMP, basomedial amygdaloid nucleus; CeM, central amygdaloid nucleus, medial division; DEn, dorsal endopiriform nucleus; LA, lateral amygdaloid nucleus; LEnt, lateral entorhinal cortex; MeA, medial amygdaloid nucleus, anterior part; MeP, medial amygdaloid nucleus, posterior part; Pir, piriform cortex; PMCo, posteromedial cortical amygdaloid nucleus.

Fig. 3. HDB and VP/SI innervate different parts of the medial prefrontal cortex.
(A, C) Images taken from different prefrontal cortical planes showing cholinergic projections from the HDB (A) and VP/SI (C) (injection sites presented in Fig. 2). Scale bar: 500 µm.
(B, D) Overlaid representative cholinergic projections from the HDB (B) and VP/SI (D). Axons represented in different colors were obtained from different animals (n=3). Maps of the prefrontal cortex were based on the mouse brain atlas (Paxinos et. al., 2004).
(E) Percentage of prefrontal cortex-projecting cholinergic axons in each cortical region from the HDB and VP/SI. AI, agranular insular cortex; Cg1, cingulate cortex, area 1; Cg2, cingulate cortex, area 2; DP, dorsal peduncular cortex; IL, infralimbic cortex; LO, lateral orbital cortex; M1, primary motor cortex; M2, secondary motor cortex; MO, medial orbital cortex; PL, prelimbic cortex; VO, ventral orbital cortex

Fig. 4. Retrograde-anterograde viral tracing reveals the presence of a cholinergic neuronal population with dual projection to the mPFC and amygdala.
(A1) A fluorescent image of cholinergic fibers in the mPFC originating from the HDB. Scale bar: 500 µm. Inset: an image taken at higher magnification shows cholinergic axons in the PL/Cg1. Scale bar: 100 µm.

(A2) Schematic representation of anterograde Cre-dependent axonal labeling. 30 nl AAV8.CAG.Flex.GFP was injected into the HDB in ChAT-Cre mice (n=3). Orange arrows indicate cholinergic axon fibers from the HDB towards the mPFC and BLA.
(A3) A fluorescent image of cholinergic fibers in the BLA originating from the HDB. Scale bar: 500 µm. Insets: images taken at higher magnification of cholinergic axons in the BMA and BA. Note the lack of axons in the BA. Scale bar: 100 µm.
(B1) A fluorescent image of cholinergic fibers in the mPFC originating from the VP/SI. Scale bar: 500 µm. Inset: an image taken at higher magnification from the dense cholinergic innervation in the PL/Cg1. Scale bar: 100 µm.
(B2) Schematic representation of anterograde Cre-dependent axonal labeling. 30 nl AAV8.CAG.Flex.GFP was injected into the VP/SI in ChAT-Cre mice (n=4). Dark blue arrows indicate cholinergic axon fibers from the VP/SI towards the mPFC and BLA.
(B3) A fluorescent image of cholinergic fibers in the BLA originating from the VP/SI. Scale bar: 500 µm. Insets: images taken at higher magnification of cholinergic axons in the BA and BMA. Note the lack of axons in the BMA. Scale bar: 100 µm.
(C1) A fluorescent image of cholinergic collaterals of BLA-projecting cholinergic cells in the mPFC. Scale bar: 500 µm. Inset: an image taken at higher magnification showing some cholinergic axons in the PL/Cg1. Scale bar: 100 µm.
(C2-C3) Schematic representation of retrograde- anterograde Cre-dependent axonal labeling. AAV5.Ef1a.DIO.eYFP was injected either into the BLA (2 x 100 nl; C_2) or mPFC (3 x 100 nl; C_3) in ChAT-Cre mice (n = 2-2). Green arrows show retrograde spread of the Cre- dependent virus into BF cholinergic cells. Black arrows indicate anterograde labeling towards the injection site. Medium blue arrow refers to anterograde labeling towards the PL/Cg1. Wine arrow points to anterograde labeling towards the IL. Cyan arrow shows anterograde labeling towards the BA. Red arrow indicates anterograde labeling towards the BMA.
(C4) A fluorescent image of cholinergic collaterals of mPFC-projecting BF cells in the BLA. Scale bar: 500 µm. Insets: images taken at higher magnification showing some cholinergic axons in the BA and BMA. Scale bar: 100 µm.
(C5) A fluorescent image of retrogradely labeled BF cholinergic cells from BLA using retrograde-anterograde viral tracing in ChAT-Cre mice. Scale bar: 500 µm.

(C6) A fluorescent image of retrogradely labeled BF cholinergic cells from the mPFC using retrograde-anterograde viral tracing in ChAT-Cre mice. Scale bar: 500 µm. ac, anterior commissure.
(D) Normalized axonal fluorescent intensity (AU) graph comparing the strength of anterograde and retrograde-anterograde innervation in the mPFC and amygdala. BA, basal amygdala; PL, prelimbic cortex; Cg1, cingulate cortex; BMA, basomedial amygdala, anterior part; IL, infralimbic cortex.

Fig. 5. Cholinergic axon terminals in the BA co-express VGLUT3 but not VGAT.
(A) Cholinergic (A1; green) and VGLUT3-containing axon terminals (A2; red) revealed by immunostaining showing high co-occurrence of VGLUT3 in cholinergic boutons in the BA (A3). Scale bar: 3 µm. Light blue arrows point to ChAT/VAChT-containing boutons. Orange arrows indicate VGLUT3 boutons. White dotted circles label double labeled i.e. cholinergic and VGLUT3 immunostained boutons.
(B) Cholinergic (B1; green) and VGLUT3-containing axonal boutons (B2; red) form largely non-overlapping populations in the BMA. Scale bar: 3 µm.
(C) Cholinergic (C1; green) and VGAT-containing axon terminals (C1) showing non-overlapping populations in the BA (C3). Scale bar: 3 µm. Light blue arrows show ChAT/VAChT-containing boutons. Dark blue arrows point to VGAT-immunoreactive boutons.
(D) Graph showing that VGLUT3 content in cholinergic axon terminals is the highest in the anterior BA (BAa; 64.8 ± 8.35%; n=3, 332/512) and posterior BA (BAp; 29.67 ± 3.51%, n=3, 89/300), while the co-expression is much lower in surrounding amygdala nuclei: LA (5.82 ± 6.33%, n=2, 17/292), BMA (2.38 ± 0.68%, n= 2, 6/252), PMCo (6.85 ± 4.93%, n=2, 24/350), Pir (2.57 ± 1.05%, n=2, 8/311), CeM (1.69 ± 1.92%, n=2, 3/177). (E) An image taken at low magnification from ChAT/VAChT (E1; green) and VGLUT3 (E1; red) immunostained sections showing high expression levels for these proteins in the BA, but not in surrounding amygdala regions. Scale bar: 500 µm.

Fig. 6. Cholinergic cells in the HDB and VP/SI express VGAT during development, but not in adult mice.

(A, B) Visualizing GABAergic cells in the HDB (A1) and VP/SI (B1) of the BF in VGAT-ZsGreen1 offspring generated by the crossing of VGAT-IRES-Cre and CAG-LSL-ZsGreen1 mice. Scale bar: 50 µm. Insets: images taken at higher magnification of a GABAergic BF neuron containing ChAT enzyme. Scale bar: 5 µm. (C, D) Viral labeling of GABAergic cells in the HDB (C1) and VP/SI (D1) by injecting AAV8.CAG.Flex.GFP into VGAT-Cre mice. Scale bar: 50 µm. Insets: images taken at higher magnification showing GABAergic and cholinergic cells intermingled in the BF. Scale bar: 5 µm.

(A2, B2, C2, D2) ChAT immunostaining revealing cholinergic cells in the BF. Scale bar: 50 µm.

(A3, B3) Merged images showing co-expression of VGAT and ChAT both in the HDB and VP/SI in VGAT-ZsGreen1 mice. Scale bar: 50 µm.

(C3, D3) Merged images showing that cholinergic cells in the HDB and VP/SI do not contain VGAT in AAV injected VGAT-Cre mice. Scale bar: 50 µm.

(E) Percentage of VGAT-expressing cholinergic cells in the HDB (Dark green, 96.7%, 546/563, n=3) and VP/SI (Dark green, 58.8%, 137/233, n=3) in VGAT-ZsGreen1 mice and AAV-injected VGAT-Cre (Light green, HDB: 3.06%, 19/620; VP/SI: 1.19%, 3/253, n=3) mice.

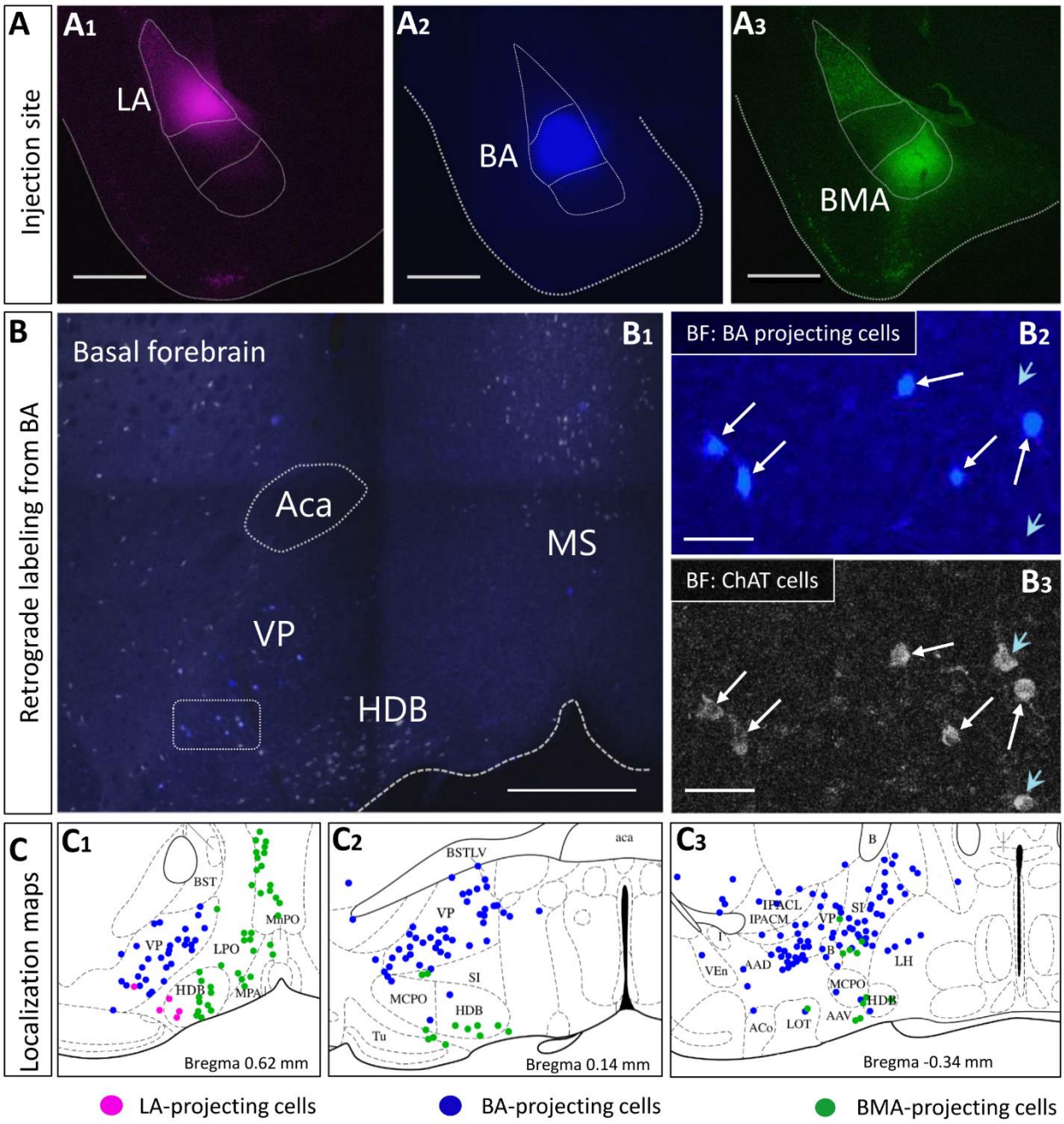
A
Injection site
A1
LA
A2
BA
A3
BMA
B
Retrograde labeling from BA
Basal forebrain
B1
Aca
MS
VP
HDB
BF: BA projecting cells
B2
BF: ChAT cells
B3
C
Localization maps
C1
BST
MnPO
VP
LPO
HDB
MPA
Bregma 0.62 mm
C2
BSTLV
aca
VP
SI
MCPO
HDB
Tu
Bregma 0.14 mm
C3
B
IPACL
IPACM
VP
SI
I
AAD
B
LH
VEn
MCPO
HDB
ACo
LOT
AAV
Bregma -0.34 mm
LA-projecting cells
BA-projecting cells
BMA-projecting cells

Figure 1

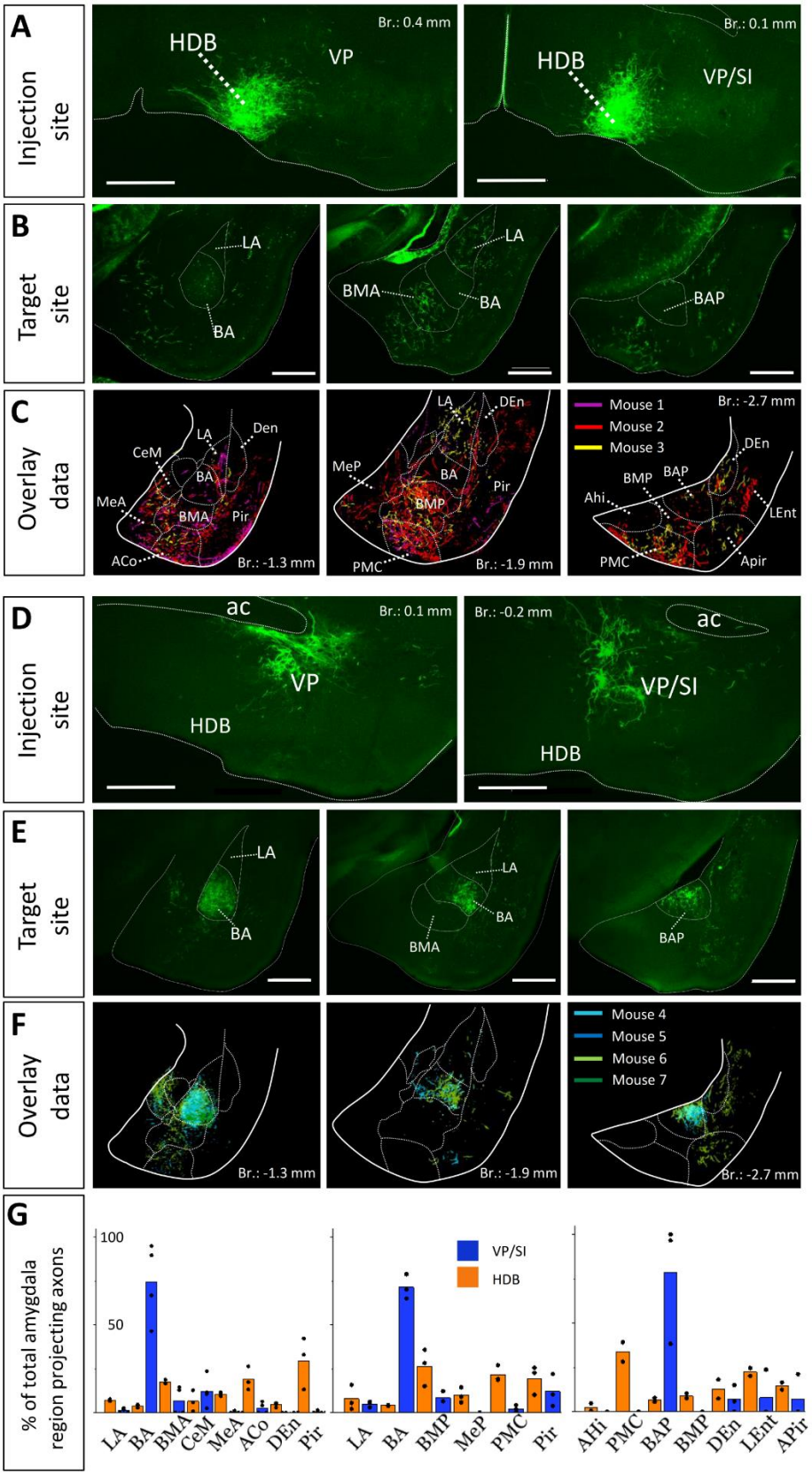
A
Injection site
Br.: 0.4 mm
HDB
VP
Br.: 0.1 mm
HDB
VP/SI
B
Target site
LA
BA
LA
BMA
BA
BAP
C
Overlay data
LA
Den
CeM
BA
MeA
BMA
Pir
ACo
Br.: -1.3 mm
LA
DEn
MeP
BA
Pir
BMP
PMC
Br.: -1.9 mm
Mouse 1
Mouse 2
Mouse 3
Br.: -2.7 mm
DEn
BMP
BAP
Ahi
LEnt
PMC
Apir
D
Injection site
ac
Br.: 0.1 mm
VP
HDB
Br.: -0.2 mm
ac
VP/SI
HDB
E
Target site
LA
BA
LA
BA
BMA
BAP
F
Overlay data
Br.: -1.3 mm
Br.: -1.9 mm
Mouse 4
Mouse 5
Mouse 6
Mouse 7
Br.: -2.7 mm
G
% of total amygdala region projecting axons
100
50
VP/SI
HDB
LA
BA
BMA
CeM
MeA
ACo
DEn
Pir
LA
BA
BMP
MeP
PMC
Pir
AHi
PMC
BAP
BMP
DEn
LEnt
APir

Figure 2

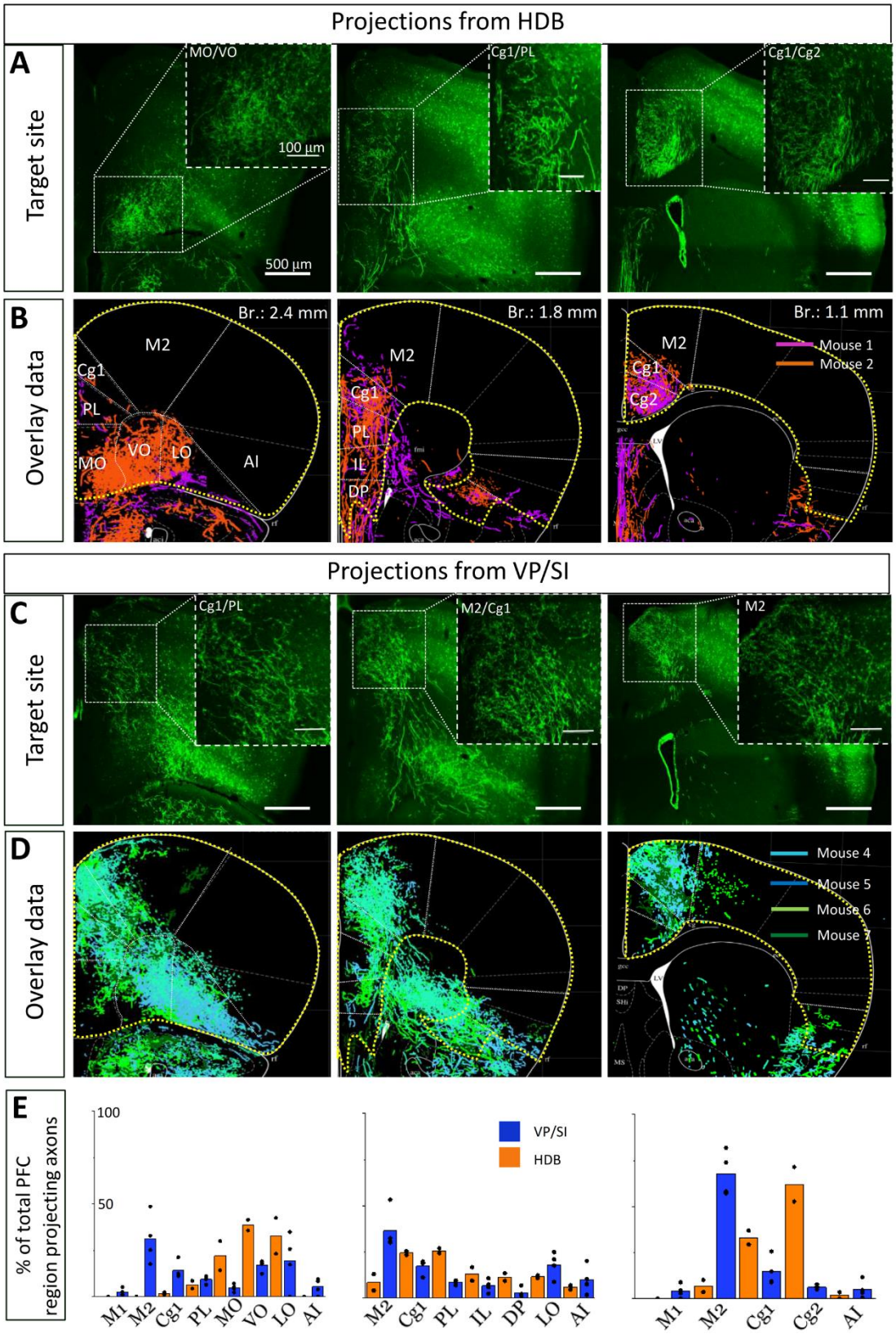
Projections from HDB
A
Target site
MO/VO
100 µm
500 µm
Cg1/PL
Cg1/Cg2
B
Overlay data
Br.: 2.4 mm
M2
Cg1
PL
MO
VO
LO
AI
Br.: 1.8 mm
M2
Cg1
PL
IL
DP
Br.: 1.1 mm
M2
Cg1
Cg2
Mouse 1
Mouse 2
Projections from VP/SI
C
Target site
Cg1/PL
M2/Cg1
M2
D
Overlay data
Mouse 4
Mouse 5
Mouse 6
Mouse 7
E
% of total PFC region projecting axons
100
50
VP/SI
HDB
M1
M2
Cg1
PL
MO
VO
LO
AI
M2
Cg1
PL
IL
DP
LO
AI
M1
M2
Cg1
Cg2
AI

Figure 3

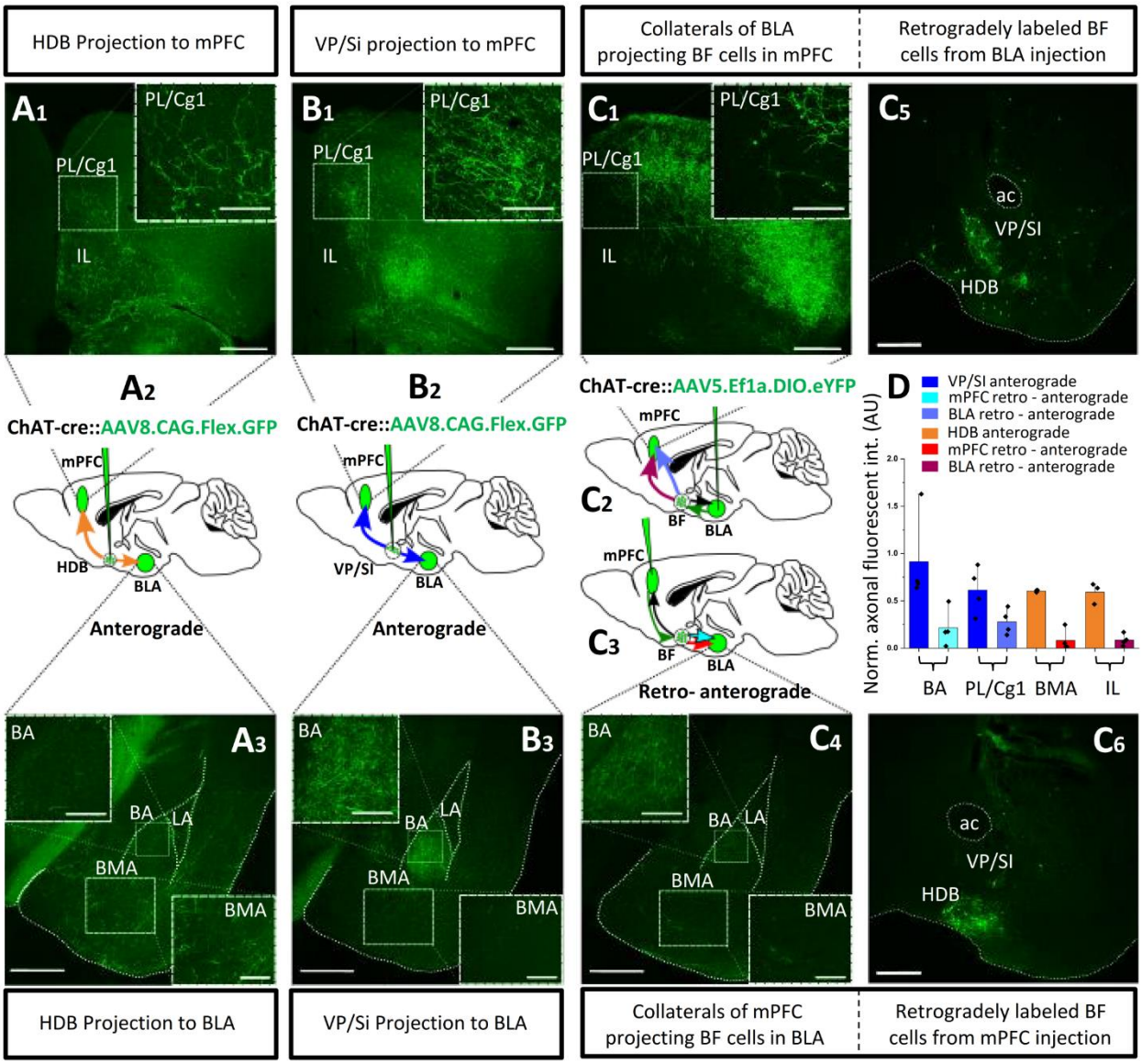
HDB Projection to mPFC
VP/Si projection to mPFC
Collaterals of BLA projecting BF cells in mPFC
Retrogradely labeled BF cells from BLA injection
A1
PL/Cg1
IL
B1
C1
C5
ac
VP/SI
HDB
A2
B2
ChAT-cre::AAV8.CAG.Flex.GFP
ChAT-cre::AAV5.Ef1a.DIO.eYFP
mPFC
HDB
BLA
VP/SI
BF
C2
C3
Anterograde
Retro- anterograde
D
VP/SI anterograde
mPFC retro - anterograde
BLA retro - anterograde
HDB anterograde
mPFC retro - anterograde
BLA retro - anterograde
Norm. axonal fluorescent int. (AU)
BA
PL/Cg1
BMA
IL
A3
B3
C4
C6
LA
HDB Projection to BLA
VP/Si Projection to BLA
Collaterals of mPFC projecting BF cells in BLA
Retrogradely labeled BF cells from mPFC injection

Figure 4

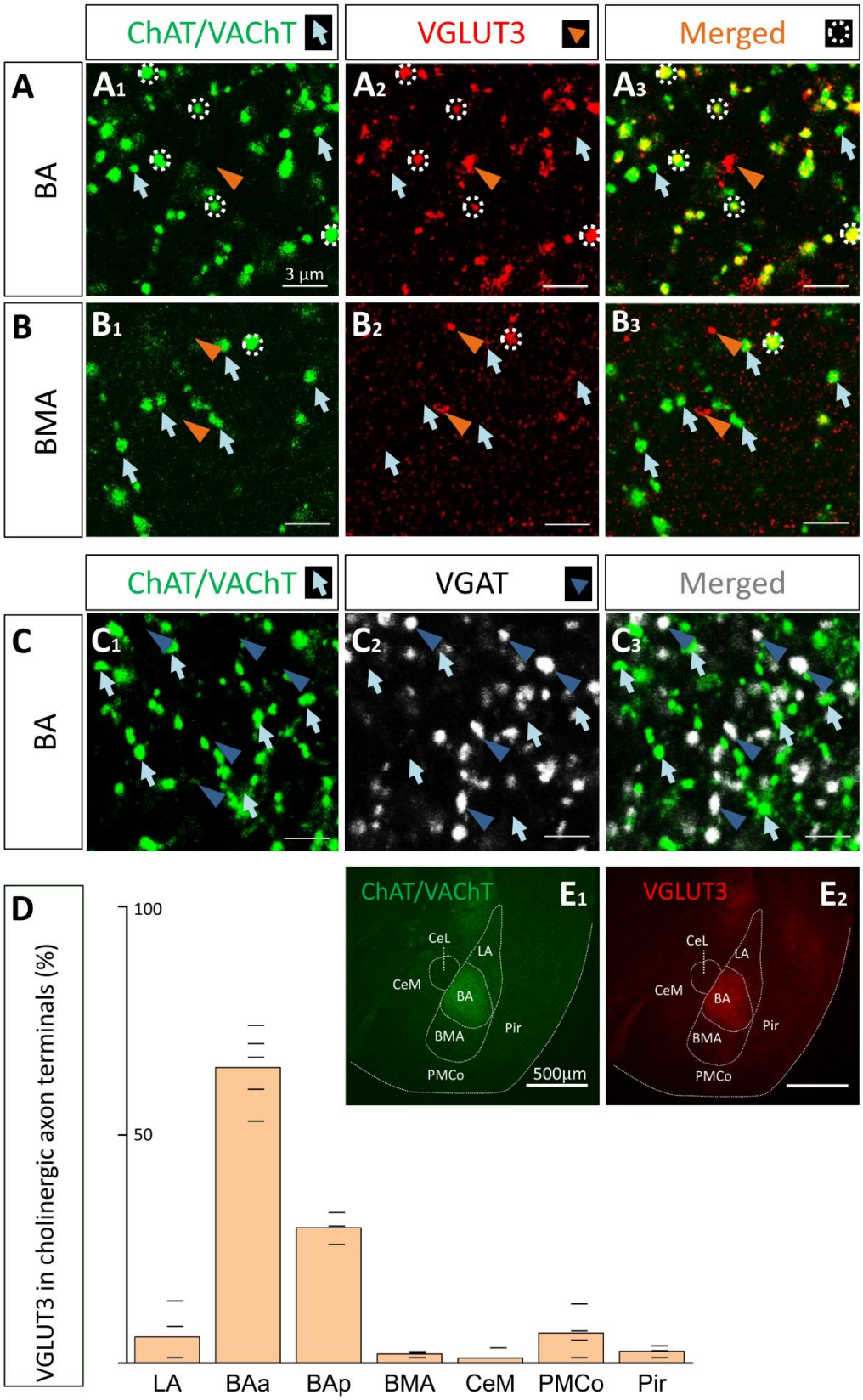
ChAT/VAChT
VGLUT3
Merged
A
BA
A1
A2
A3
3 µm
B
BMA
B1
B2
B3
ChAT/VAChT
VGAT
Merged
C
BA
C1
C2
C3
D
VGLUT3 in cholinergic axon terminals (%)
100
50
LA
BAa
BAp
BMA
CeM
PMCo
Pir
ChAT/VAChT
E1
CeL
LA
CeM
BA
BMA
Pir
PMCo
500µm
VGLUT3
E2
CeL
LA
CeM
BA
BMA
Pir
PMCo

Figure 5

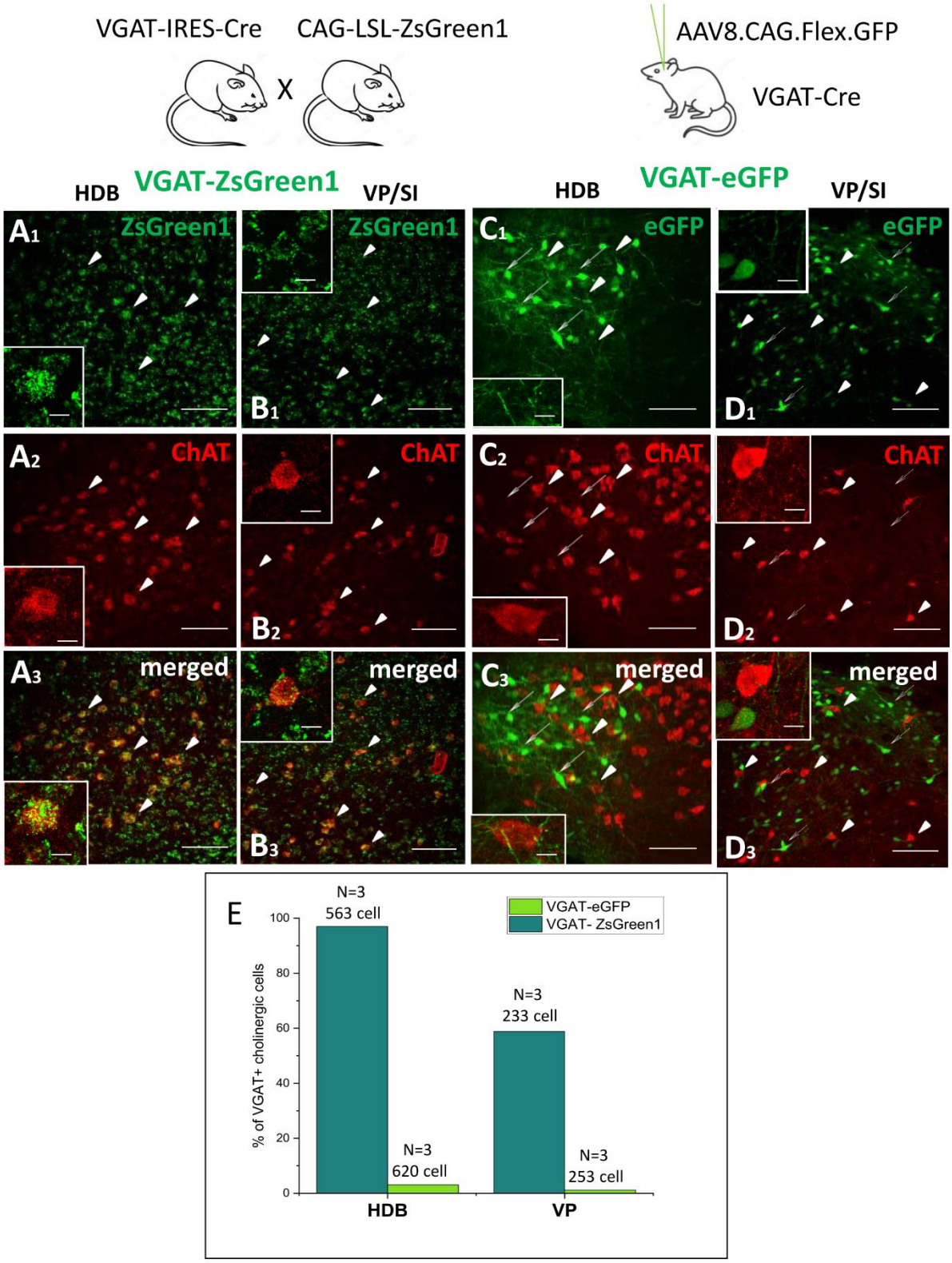
VGAT-IRES-Cre
CAG-LSL-ZsGreen1
X
AAV8.CAG.Flex.GFP
VGAT-Cre
HDB
VGAT-ZsGreen1
VP/SI
HDB
VGAT-eGFP
VP/SI
A1
ZsGreen1
B1
ZsGreen1
C1
eGFP
D1
eGFP
A2
ChAT
B2
ChAT
C2
ChAT
D2
ChAT
A3
merged
B3
merged
C3
merged
D3
merged
E
VGAT-eGFP
VGAT- ZsGreen1
% of VGAT+ cholinergic cells
100
80
60
40
20
0
N=3
563 cell
N=3
620 cell
N=3
233 cell
N=3
253 cell
HDB
VP

Figure 6